DOI: 10.13009/EUCASS2023-013
Aerospace Europe Conference 2023 – 10TH EUCASS – 9TH CEAS

Thermo-mechanical numerical model of a small-scale liquid hydrogen aircraft fuel tank

George Lampeas and George Tzoumakis
Mechanical Engineering and Aeronautics Department, University of Patras
University Campus 26500 Rion – Patras, Greece
labeas@upatras.gr – gtzoumakis@upnet.gr

Abstract
Future LH2 powered aircraft require the design of cryogenic tanks. These tanks are expected to have complex structures and loads, and therefore Finite Element thermal and structural analyses are required to assess their performance, while design optimization demands the investigation of several concepts. The present work sets the framework for the development of a parametric thermo-mechanical model of a small-scale liquid hydrogen aircraft fuel tank, conducting FE thermal analysis, followed by FE structural analysis.
This work is related to FLHYing tank (flight demonstration of a Liquid HYdrogen load-bearing tank in an unmanned cargo platform), funded by HORIZON-JU-CLEAN-AVIATION.

1. Introduction

With global temperatures rising and the effects of climate change evident, there is an increasing demand for the use of more sustainable energy sources. With the transport segment responsible for about one-third of the total CO_2 emissions in the European Union, alternative fuels are investigated. Hydrogen is a promising alternative fuel as when produced carbon-free any CO_2 emissions are eliminated. Its usage in fuel cells allows for zero-emission propulsion. When burnt in an internal combustion engine, exceptionally low particle emissions can be expected, as well as reduced NOx emissions, provided that the combustion system is optimized.

Hydrogen is exceptionally attractive as an aviation fuel due to its high heating value, as it has about 2.8 times more energy per mass unit compared to conventional fuels. However, the extremely low density of hydrogen causes serious storage issues. Hydrogen is usually stored compressed at 350-700 bar, or in liquid form, at a temperature of -253 ºC. Liquid hydrogen (LH2) has a significantly higher density than compressed, rendering it the most viable solution for aircraft. Several projects like the Airbus Cryoplane have investigated the transition to LH_2 powered aircraft with promising predictions, but liquid hydrogen is not yet a proven aviation fuel, as only a handful of prototypes like the Tupolev Tu-155 have been built and tested.

As the LH_2 powered aircraft technologies are not yet fully developed, the investigations should start with small scale applications. Several parts of the fuel system have to be designed, with the liquid hydrogen tank being the largest part and with conflicting design requirements. It has to demonstrate low heat losses in order to prevent the cryogenic fuel from boiling off, it has to be capable of bearing several mechanical and thermal loads, while keeping weight to the minimum. In this direction, the present work refers to the design and modeling of a small scale LH_2 tank with a capacity of ~1000 lt. Although several materials could be considered for the structural parts, aluminum alloy 2219 is selected, a material used for LH_2 tank construction since the 1960s during the Apollo program. The supporting structure of the inner tank should be capable of bearing mechanical loads while being an efficient insulator. For the supports the selected material is PEEK, a thermoplastic with high strength and low thermal conductivity. Silica aerogel is selected for the insulation, a material with extremely low thermal conductivity.

The cryogenic tanks are expected to be stiffened by internal members such as stringers, frames, and stiffeners, typical structural components of aircraft. Various thermal and mechanical operational loads are applied simultaneously, in various combinations. The complex geometry and different types of loads lead to numerous design parameters being considered for a cryogenic aviation tank. Therefore, the design process should be heavily based on parametric numerical simulations.

DOI: 10.13009/EUCASS2023-013

In this direction, a thermo-mechanical simulation methodology is developed for metallic cryogenic hydrogen tanks. The model consists of a thermal module and a structural module. The thermal module conducts heat transfer analysis in order to calculate the temperature distribution and the heat losses. The structural module uses the results of the thermal module as an input and combines the thermal and mechanical loads in order to conduct stress, strain and displacement calculations. The FE model combines solid elements with thin-shell and beam elements, with both geometry and loads being parametric, enabling studies for different tank variations like variable wall thickness, insulation thickness, supporting structure geometry etc. The developed model can be used to assess the structural and thermal performance of the tank and its overall efficiency as function of its sizing parameters.

The geometry and materials used in the tank model development are described in chapter 2. In chapters 3 and 4, details of heat transfer and structural analyses and their corresponding loads, boundary conditions and results are presented. Conclusions and future work proposals are provided in the 5th and final section.

2. The small-scale liquid hydrogen fuel tank description

The multi-parametric model developed allows the creation of radially symmetric tanks of different geometries. The supporting structure can also be adapted as needed. Almost every design aspect is a changeable parameter, simplifying design revision or different design creation without major changes in the model.
For the present analysis, an independent cylindrical tank with elliptical domes is considered. Total length of the inner tank is 1.5 m with a maximum diameter of 1 m. The tank has an internal volume of 1046 lt. Considering a 3% ullage, the maximum LH_2 capacity is 1015 lt or 71.9 kg of liquid hydrogen assuming an average density of 70.85 kg/m^3. A 15 cm thick layer of silica aerogel insulation is placed between the two walls, meaning that the outer tank has a length of 1.8 m with a maximum diameter of 1.3 m. The two tanks are made from aluminum alloy 2219, with the inner tank having a thickness of 1 mm and the outer 0.5 mm.

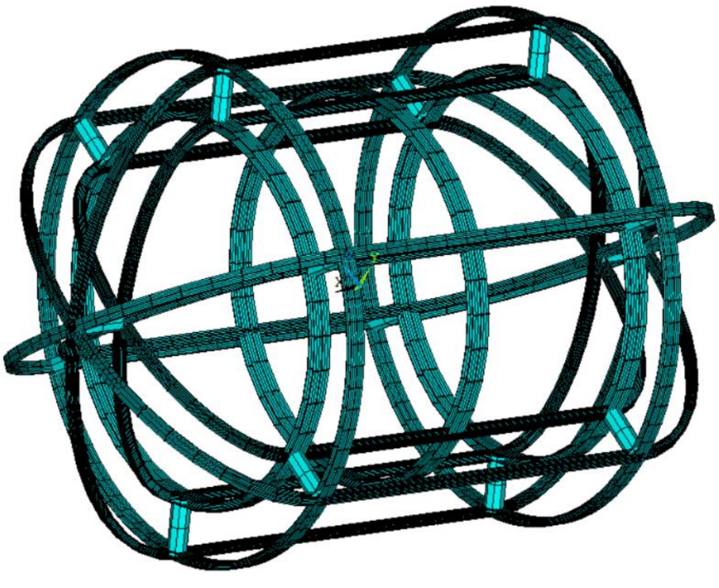

Figure 1: Supporting and Stiffening Structure of the Modeled Tank

Both tanks are stiffened by 6 longitudinal beams. The outer tank is stiffened by 2 rings while the inner tank is stiffened by 3 rings due to the higher load of the overpressure. All beams are made of aluminum alloy 2219 and have an I cross section, with the geometric characteristics presented in the following table.

Table 1: Geometrical characteristics of the stiffening members

		Flange width (mm)	Flange thickness (mm)	Web depth (mm)	Web thickness (mm)
Inner tank	Rings	50	2	25	2
	Beams	25	2	25	2
Outer tank	Rings	40	2	20	2
	Beams	30	2	20	2

DOI: 10.13009/EUCASS2023-013

The inner tank is supported by 14 PEEK tubes of 50 mm in diameter and 0.5 mm in thickness.

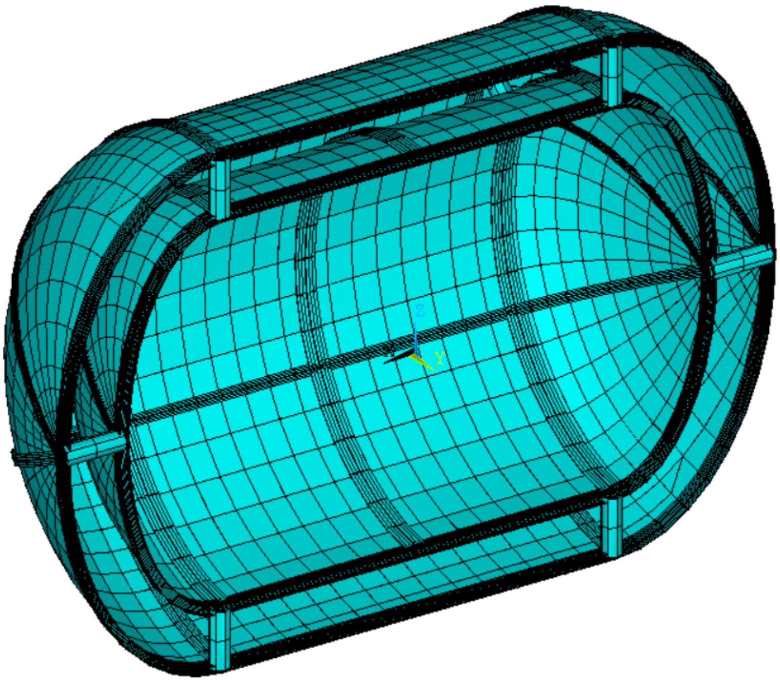

Figure 2: Cutaway of the Modeled Tank Showing the Tank Walls and the Supporting Structure

The temperature dependent material properties that the model uses as input are summarized in the following table.

Table 2: Material Properties of the tank and the insulation materials for a range of 20-300K [1][2][3]

	Aluminum 2219-T62	**PEEK**	**Silica Aerogel**
Density (293 K)	2840 kg/m^3	1320 kg/m^3	71 kg/m^3
Thermal Conductivity	31-126 W/mK	0.0659-0.2821 W/mK	$1.55 \cdot 10^{-4}$-$3 \cdot 10^{-3}$ W/mK
Thermal Expansion Coefficient	$14.4 \cdot 10^{-6}$-$22.5 \cdot 10^{-6}$ K^{-1}	$12.5 \cdot 10^{-6}$-$40.1 \cdot 10^{-6}$ K^{-1}	$4.2 \cdot 10^{-6}$-$10.08 \cdot 10^{-6}$ K^{-1}
Specific Heat Capacity	340-864 J/kgK	241-1081 J/kgK	45-1500 J/kgK
Modulus of Elasticity	79-73.1 GPa	6.8-3.5 GPa	3.33-2.22 MPa
Poisson's Ratio	0.33	0.38	0.24

DOI: 10.13009/EUCASS2023-013

3. Heat Transfer Analysis

The analysis starts by modelling and meshing the geometry. The tank walls are meshed with 2D 4-node shell elements, the supporting structure is meshed with 1D 2-node link elements and the insulation is meshed with 3D 8-node solid elements, all with temperature degrees of freedom. The thermal loads and boundary conditions depend on the environmental conditions inside the fuselage part where the tank is placed and on the inner tank cryogenic conditions. Although not always defined, some accurate assumptions can be used for the heat transfer analysis. The process for heat transfer analysis, thermal design evaluation and boil-off rate (BOR) calculation is described below. Heat transfer within the tank and its surrounding structure depends on thermal conduction, thermal convection, and to a lesser extent to thermal radiation. The thermal analysis methodology is summarized in the following figure.

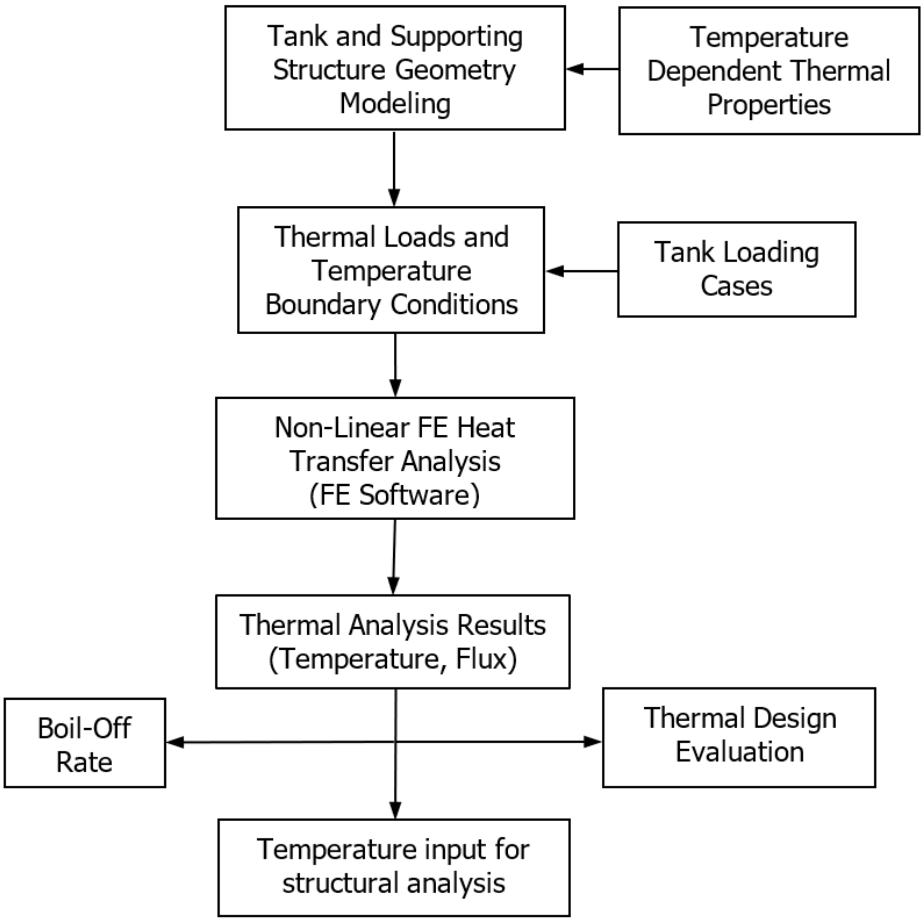

Figure 3: FE Thermal Analysis Process

The thermal analysis is non-linear, as the thermal properties are a function of temperature. This process demands computational power but produces more accurate results. Temperature distribution results of the thermal analysis are stored and subsequently used as an input for the structural analysis.

3.1 Thermal Loads

The main thermal load is convective heat transfer from the air to the outer tank surface. Thermal convection is a heat transfer mechanism based on movement of molecules within fluids such as gases and liquids. Convective heat transfer is classified into two types: free convection and forced convection. Free (natural) convection occurs when the flow is induced by buoyancy forces arising from density differences within the fluid. Forced convection is caused by relatively fast external flows. Slower flows induce a mixed mechanism of natural and forced convection. As the LH_2 tank is assumed completely enclosed into the aircraft fuselage, forced convection is not the case in the present heat transfer analysis. The heat loads are calculated using semi-empirical correlations [4].

DOI: 10.13009/EUCASS2023-013

The heat transfer in a free convection boundary layer depends on the relative magnitude of buoyancy and viscous forces in the fluid. Its occurrence is generally correlated in terms of the Rayleigh number (Ra) and the Nusselt (Nu) number. The Rayleigh number is a product of the Grashof (Gr) number and the Prandtl (Pr) number. The Nusselt number (which is defined as a function of Rayleigh number) provides a measure of the convection heat transfer occurring at the surface. The Rayleigh number is expressed in the following equation:

$$\mathrm{Ra_L} = \mathrm{Gr_L Pr} = \frac{g\beta(T_s - T_b)L_c^3}{\nu^2} \qquad \textbf{(1)}$$

where:
g = gravity acceleration
β = thermal expansion coefficient of the bulk fluid at the average temperature
ν = kinematic viscosity of the bulk fluid at the average temperature
T_s = surface temperature
T_b = bulk fluid temperature
L_c = critical length of the surface
The convection coefficient is expressed as a function of the Nusselt number in the following equation:

$$h = \frac{Nuk}{L_c} \qquad \textbf{(2)}$$

where:
k = thermal conductivity of the bulk fluid

The Nusselt number calculation equation differs significantly for different geometries, yet the Nusselt number can be empirically calculated for the most common ones.

For the cylindrical body, the empirical equation for Horizontal cylinders is used. The critical length in this case is the radius of the cylinder. The Nusselt number is expressed in the following equation:

$$Nu = \left\{0.6 + \frac{0.387Ra^{1/6}}{\left[1+(0.599/Pr)^{9/16}\right]^{8/27}}\right\}^2 \qquad \textbf{(3)}$$

For the elliptical domes, the empirical equation for spheres can yield adequate results. The critical length is the average of the major and minor semi-axes. The Nusselt number is expressed in the following equation:

$$Nu = 2 + \frac{0.589Ra^{1/4}}{\left[1+(0.469/Pr)^{9/16}\right]^{4/9}} \qquad \textbf{(4)}$$

As far as thermal radiation is concerned, as the temperature of the outer tank is assumed to be similar to that of the surrounding parts of the fuselage, the heat transfer due to radiation can be ignored.

3.2 Thermal Boundary conditions

The surface of the inner tank which is in contact with the liquid hydrogen is assumed to have the same temperature as the liquid. Therefore, any inner tank wall nodes bellow the liquid hydrogen surface are given a temperature boundary condition of the liquid hydrogen boiling temperature for the given pressure.

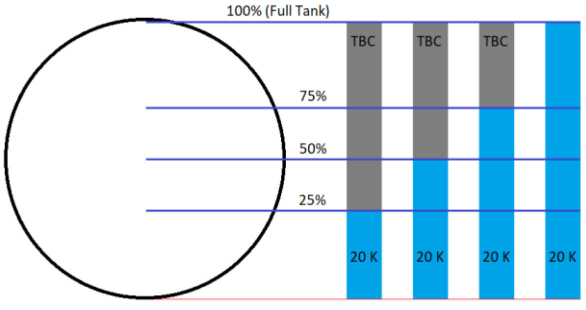

Figure 4: Temperature Boundary Conditions for Different Load Cases for 1 bar

DOI: 10.13009/EUCASS2023-013

3.3 Thermal analysis results

3.3.1 Heat Flux

Heat flux is the amount of heat energy that is transferred through a given area per time. High heat flux is an indication of poor insulation and high thermal losses. Results are presented in the following figures.

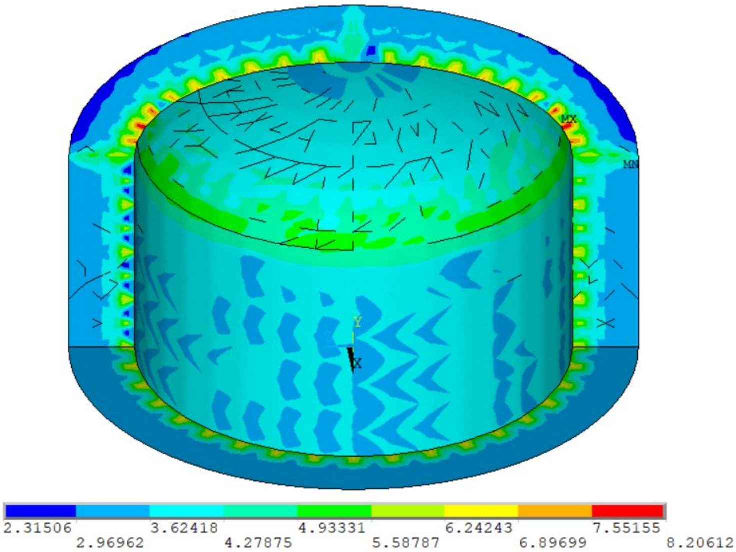

Figure 5: Heat Flux Distribution Within the Insulation for full filling (units in W/m^{2}K)

The lowest heat flux values are observed on the elliptical part, as it has the lowest convection coefficient. Significantly increased heat flux values can be observed around the supporting structure that has higher thermal conductivity than the insulation.

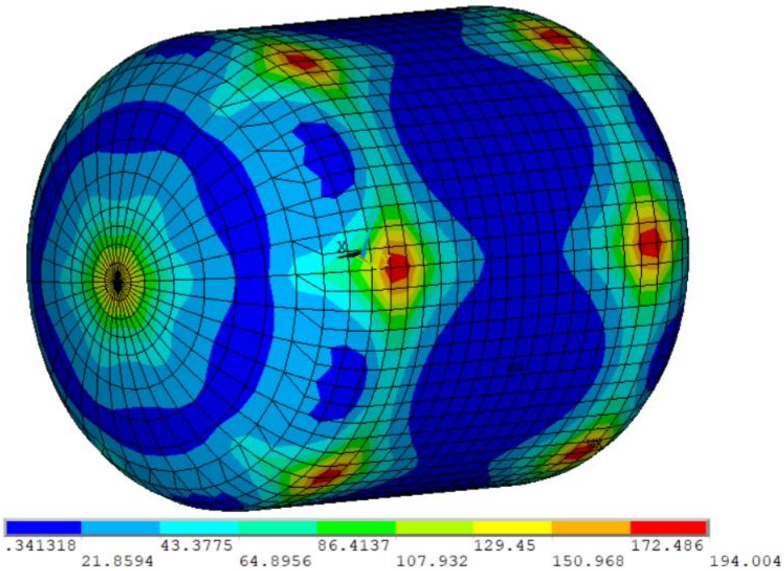

Figure 6: Heat Flux Distribution the Outer tank for full filling (units in W/m^{2}K)

The increased cross section area of the stiffening members of the outer tank are also contributing to the thermal losses as increased heat flux can be observed around them.

DOI: 10.13009/EUCASS2023-013

3.3.2 Boil-off Rate

The heat flux into the hydrogen tank generates boil-off gas. This results in pressure increase inside the tank and the excess gas needs to be released to maintain maximum design pressure. Therefore, it is necessary to assess the BOR in order to assess the insulation system. The daily BOR can be estimated by the following equation:

$$BOR = Q / (\rho H V) \times 3600 \times 24 \times 100\% \quad \textbf{(5)}$$

where :
Q = total heat flux from outside to inside tank
ρ = fluid density
V = tank volume capacity
H = latent heat for vaporization

The reaction solution of the model calculated a heat flow of 28.95 W. Given the latent heat for vaporization of hydrogen is 461 KJ/kg, the calculated boil off rate is 7.29% per day.

3.3.3 Temperature Distributions

Temperature distributions can be used to assess the efficiency of the insulation and it are an input of the following structural analysis. Temperatures on the outer tank wall should be close to ambient in order to avoid ice formation or water vapor condensation. Temperature gradients induce thermal stresses and therefore should be minimized.

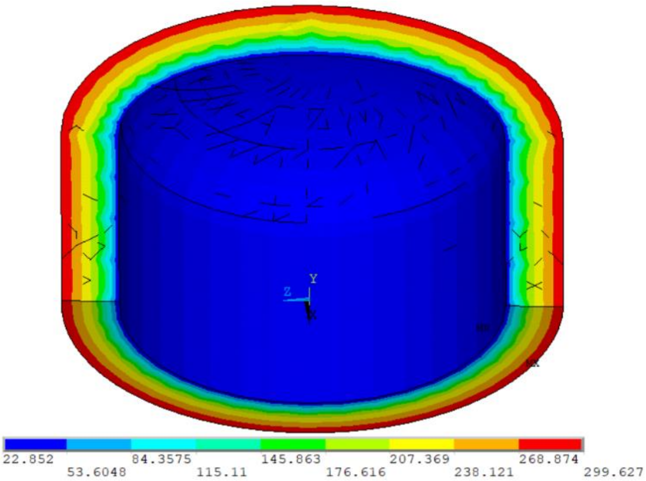

Figure 7: Temperature Distribution within the insulation for full filling (units in K)

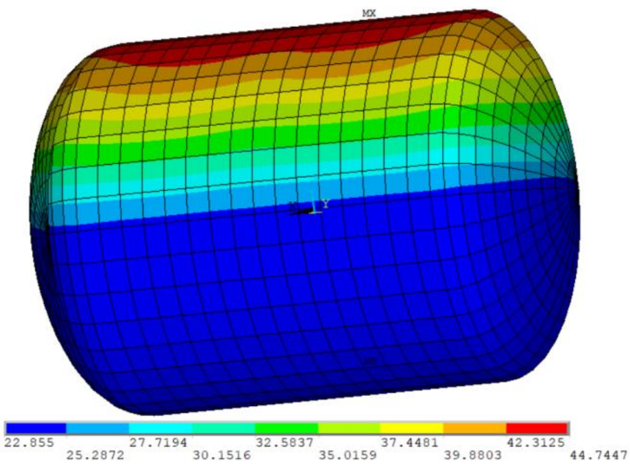

Figure 8: Temperature Distribution on the Inner Tank for 50% filling (units in K)

DOI: 10.13009/EUCASS2023-013

4. Structural Analysis

The structural analysis starts by remeshing the geometry. The tank walls are meshed with 2D 4-node shell elements, the supporting structure is meshed with 1D 2-node beam elements and the insulation is meshed with 3D 8-node solid elements, all with displacement degrees of freedom. Displacement boundary conditions are applied where the tank is externally supported. Structural loads are applied and the temperature results from the heat transfer analysis are applied to the structural model for the calculation thermal strain and the definition of the mechanical properties to be used by the model. The thermal analysis methodology is summarized in the following figure.

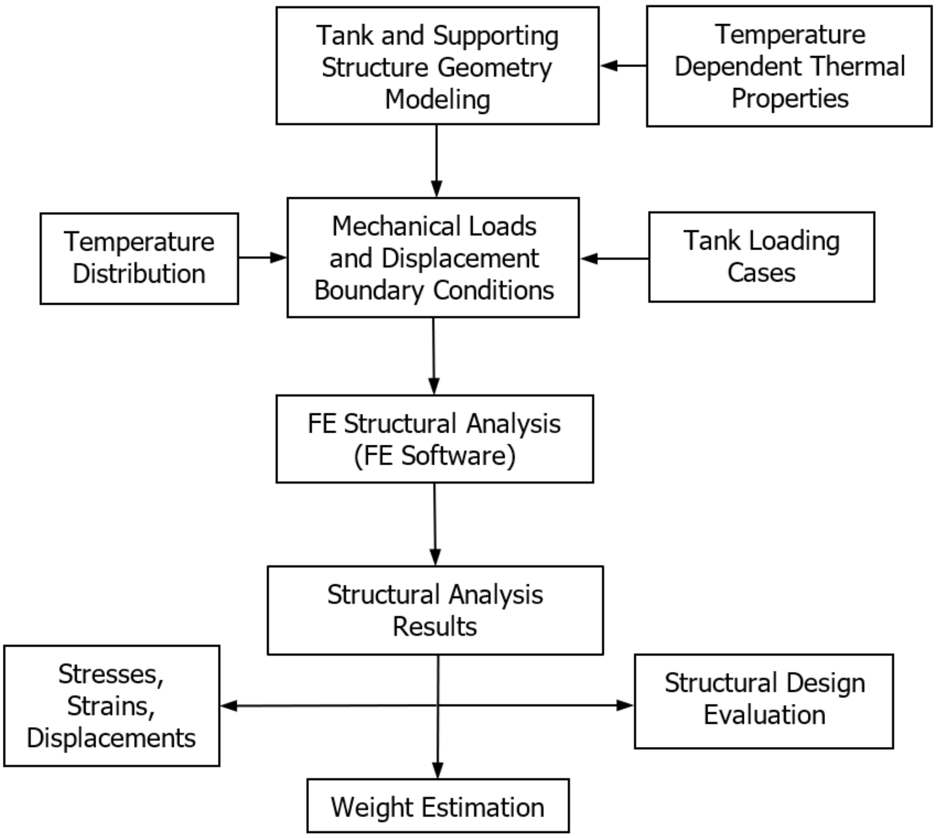

Figure 9: FE Structural Analysis Process

Structural analysis is the final module of the model, producing results that are used to verify the structural integrity of the tank. Stress and strains are used to identify potential failure of the structural materials while displacements are used to evaluate the rigidity of the structure and any potential interactions with other non-modeled parts of the aircraft.

4.1 Structural Loads

The results of the thermal analysis are used as an input for the definition of the temperature dependent mechanical properties as well as the calculation of thermal expansion/contraction displacements and loads. The tanks is assumed to be built at a temperature of 20 °C, and thus the reference temperature is set at 293 K.

The main structural load is the internal pressure. The operating pressure of the tank is 2 bar, meaning that the proof pressure should be 3 bar and the burst pressure should be 4 bar. This means that there should not be any kind of failure at 3 bar and it should not fail in a catastrophic manner until above 4 bar. Therefore, the inner tank stress multiplied by 1.4 should not exceed the yield strength for a 3 bar pressure and it should not exceed the ultimate strength for a 4 bar pressure [5]. For each load case pressure is applied to the inner tank wall elements as a surface load.

Every element is given mass according to its volume and material. Acceleration is applied as a load to the whole model and the inertia loads can be calculated accordingly.

DOI: 10.13009/EUCASS2023-013

The interaction between the tank wall and the fluid is simulated by a hydrostatic pressure distribution:

$$\mathrm{P} = \mathrm{dgh} \quad \textbf{(6)}$$

where:
g = total acceleration
d = density of the fluid
h = the distance from the surface of the fluid
The plane representing the surface is parametrically calculated for each fill level and acceleration. Hydrostatic pressure is only calculated for elements below the surface of the liquid. The hydrostatic pressure is added to the internal pressure load and for each load case the combined pressure is applied to the inner tank wall elements as a surface load.

4.2 Structural Boundary Conditions

There are a 14 mounting points on the outer tank, all of them in points were the stiffening members are connected in order to reduce stress concentrations on the thin outer tank wall. Theses nodes are given 0 degrees of freedom with no displacements or rotations allowed.

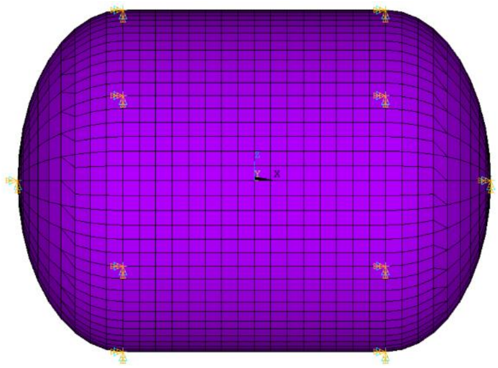

Figure 10: Structural Boundary Conditions

4.3 Structural Analysis results

As mass is assigned to all elements for inertia loads calculation, it is possible to calculate the mass of each individual component, as well as the total combined mass. The masses of all tank components are presented in the following table.

Table 3: Component Masses

Component	Mass [kg]
Inner tank wall	15.030
Inner tank stiffening structure	12.265
Outer tank wall	11.476
Outer tank stiffening structure	11.371
Supporting PEEK tubes	1.958
Insulation	70.090
Total	122.190

The gravimetric index is defined as:

$$\mathrm{GI} = \frac{mass_{LH_2}}{mass_{LH_2} + mass_{tank}} \quad \textbf{(7)}$$

The gravimetric index of the modeled tank is 0.37.

DOI: 10.13009/EUCASS2023-013

Stresses were calculated for the proof and burst pressures. For a 3 bar proof pressure the maximum stress on the inner tank was calculated at 204 MPa. With the yield strength of Al 2219 at 27 °C (300 K) being 290 MPa, the safety factor is 1.42. For a 4 bar burst pressure the maximum stress was calculated at 272 MPa. With the ultimate strength of Al 2219 at 27 °C (300 K) being 410 MPa, the safety factor is 1.51. For both proof and burst pressures the safety factor exceeds the mandated 1.4. It should also be considered that under the cryogenic operating conditions the yield and ultimate strengths of Al 2219 are significantly higher, yet the worst possible load case is considered for sizing the tank wall. Several combined load cases can be examined, with some indicative results for certain components presented in the following figures.

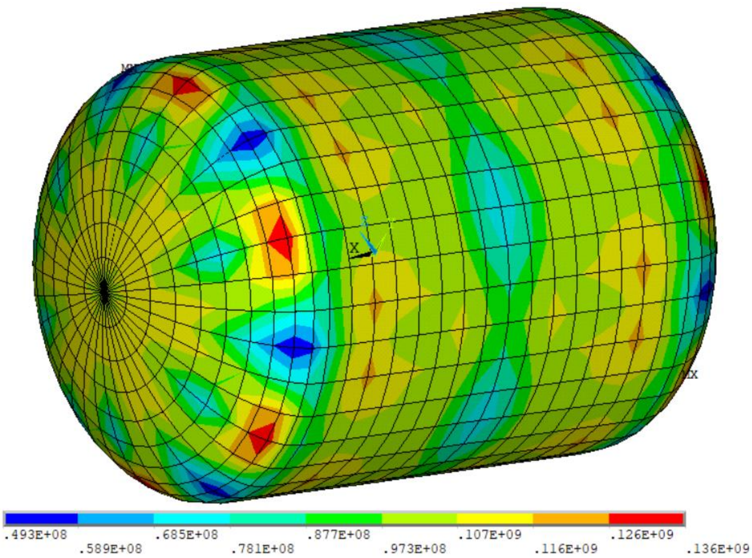

Figure 11: Inner Tank von Mises Stress for Full Loading at 2 bar During a 2 G Maneuver (units in Pa)

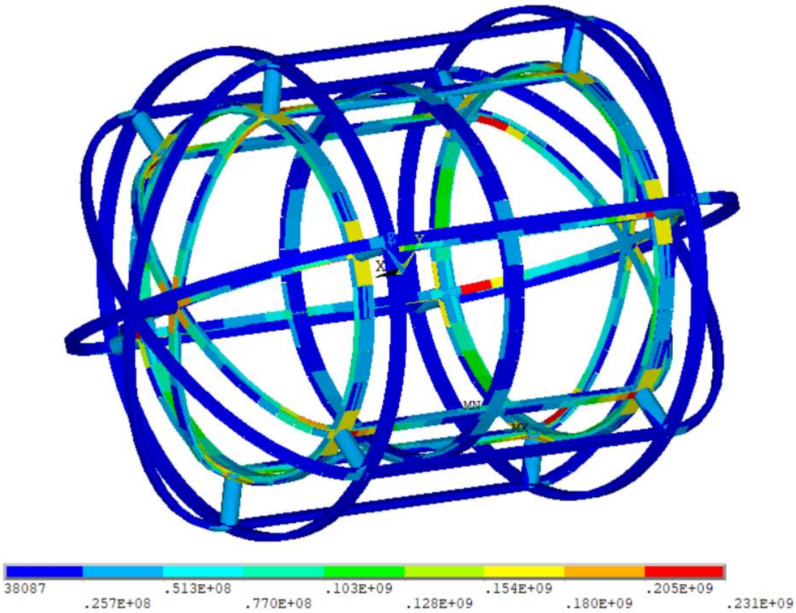

Figure 12: Stiffening Members Bending Stresses for Full Loading at 2 bar During a 2 G Maneuver (units in Pa)

DOI: 10.13009/EUCASS2023-013

Certain materials like aerogel fail under large strains. Therefore, strain distributions should also be examined.

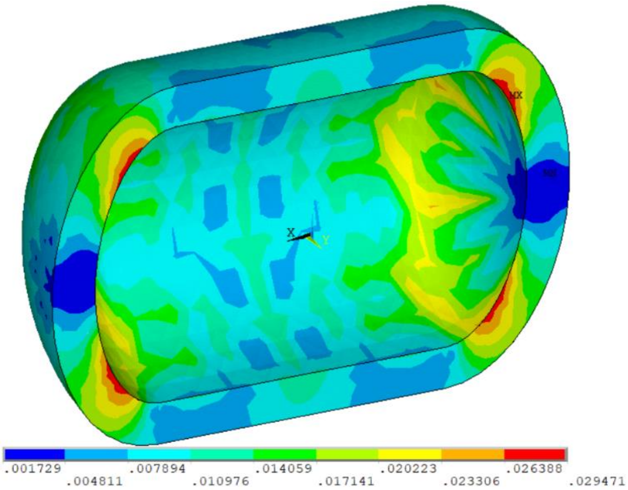

Figure 13: Insulation Strain for 50% Loading at 2 bar During a 1.5 G Maneuver

5. Conclusions and Future Work

A three-dimensional finite element model capable of simulating the operating conditions of a liquid hydrogen tank, as well as predicting temperature and stress distributions of any of the components has been developed. Major heat conduction, convection and structural loads are simulated through a finite element (FE) thermal-structural analysis. The developed model considers temperature dependent thermal and mechanical material properties. The model is parametric, allowing investigation of different design concepts and load cases. The developed numerical simulation is a useful tool for calculation of operating parameters such as boil-off rate, verification of the material selection, as well as design revision, contributing to identification of possible failures, and assessing the behavior of the tank under different operational conditions. The current model needs further development, in both the heat transfer and structural analysis parts. The thermal model may be improved by the addition of radiation heat transfer as well as the investigation of the thermal effects of boiling liquid hydrogen. The structural model may be further improved by incorporating dynamic phenomena, such as movement of the liquid hydrogen inside the tank (sloshing) during maneuvers, modeling of peripheral equipment and interactions as well as introduction of material imperfections and defects for fatigue life calculations. The model may also be adapted to simulate an integrated tank, with the outer tank modified to be a load bearing part of the fuselage. Fatigue cycles caused by combined mechanical and thermal loads can also be investigated in a future work. As the model is multi-parametric, a trade study between boil-off rate, weight, or other design aspects, can be conducted, rendering the simulation a useful tool for design revision, resulting in more efficient tanks.

Acknowledgments

The presented research has been partly funded by the HORIZON-JU-CLEAN-AVIATION-2022-01-HPA project entitled ‘flight demonstration of a Liquid HYdrogen load-bearing tank in an unmanned cargo platform’ (fLHYing tank), grant agreement number 10110146.

References

[1] Reed, R P, Purtscher, P T, Simon, N J, McColskey, J D, and Walsh, R P. Aluminum alloys for ALS cryogenic tanks: Comparative measurements of cryogenic mechanical properties of Al-Li alloys and alloy 2219, February 1993. United States: N. p., 1993

[2] Rule, D L, and Larry L. Sparks. Low-temperature Thermal Conductivity of Composites: Alumina Fiber/epoxy and Alumina Fiber/peek. Boulder, Colo: U.S. Dept. of Commerce, National Institute of Standards and Technology, 1989.

DOI: 10.13009/EUCASS2023-013

[3] P. Scheuerpflug, M. Hauck, J. Fricke, Thermal properties of silica aerogels between 1.4 and 330 K, Journal of Non-Crystalline Solids, Volume 145,1992,Pages 196-201,ISSN 0022-3093, https://doi.org/10.1016/S0022-3093(05)80455-7.

[4] Cengel, Y. A., & Ghajar, A. J. 2014. Heat and mass transfer: Fundamentals and applications (5th ed.). McGraw-Hill Professional.

[5] Standard: Space Systems—Metallic Pressure Vessels, Pressurized Structures, and Pressure Components (ANSI/AIAA S-080A-2018)